

A High Spectral Resolution Lidar Designed for Unattended Operation in the Arctic

I. A. Razenkov, E. W. Eloranta, J. P. Hedrick, R. E. Holz, R. E. Kuehn, and J. P. Garcia

University of Wisconsin-Madison
1225 West Dayton St.
Madison, WI 53706

Tel: +608-262-7327 • Fax: +608-262-0166

Email: igorR@ssec.wisc.edu

ABSTRACT

This paper describes progress in the assembly and testing of a new High Spectral Resolution Lidar (HSRL) for long-term unattended observations of arctic clouds and hazes. After a long wait for the delivery of critical components, assembly is nearly complete and some of the critical components have been tested. Most notably, the polarization based transmit-receive switch operates successfully. Atmospheric data has been acquired with the system operating as a normal backscatter lidar. The geometric overlap factor has been measured and compared to results from an optical system model.

1. THE ARCTIC HSRL

The University of Wisconsin High Spectral Resolution Lidar (HSRL) provides vertical profiles of optical depth, backscatter cross-section depolarization and backscatter phase function. All HSRL measurements are absolutely calibrated by reference to molecular scattering which is measured at each point in the lidar profile (Grund 91, Piironen 94). This enables the HSRL to measure backscatter cross-sections and optical depths without prior assumptions about the scattering properties of the atmosphere. The depolarization observations allow robust discrimination between ice and water clouds. Rigorous error estimates can be computed for all measurements.

This paper describes a compact new HSRL designed for long-term observations of arctic clouds and hazes. Unlike the current HSRL which is housed in a 46 ft semi-trailer and requires continuous attention from a highly trained operator, the new instrument is designed to operate unattended. It will operate as an Internet appliance, with operation and data transfer controlled remotely.

One of the most troublesome features of the current HSRL involves maintaining alignment of the laser beam with the receiver field of view. Alignment is sensitive to perturbations at the $10 \mu\text{rad}$ level. In the new design, this problem is avoided by employing a transceiver configuration where the transmitter and receiver share the same 0.4 m diameter telescope (Fig. 1). In addition, the large transmitter aperture limits both the per shot energy density and the multi-pulse average power density to eye-safe levels at the exit port. A passive polarization transmit-receive (T-R) switch consisting of a polarization beam splitter and a 1/4-wave plate is employed. Our first critical test was to measure the parasitic light incident on the detectors during emission of the laser pulse. The molecular channel is well protected by the combined rejection of the polarization T-R switch and the I_2 filter attenuation. The channels without the I_2 filter received excessive illumination. It was necessary to include central beam blocks in both the transmitted beam and in the received light path in order to prevent illumination of (and to mask reflections from) the central part of the telescope secondary mirror (see fig 1). Without these, transmitted light incident on the center of the telescope secondary is reflected directly to the detectors. Preliminary testing with the beam blocks installed indicates that stray light is sufficiently attenuated so that the atmospheric returns are unaffected.

The etalon filter used in the current HSRL employs a flow through N_2 pressure regulation system for tuning which is not suitable for unattended operation. Pressure tuning of the etalon in the new system is accomplished using a stepper-motor driven bellows. Flowing N_2 is not required.

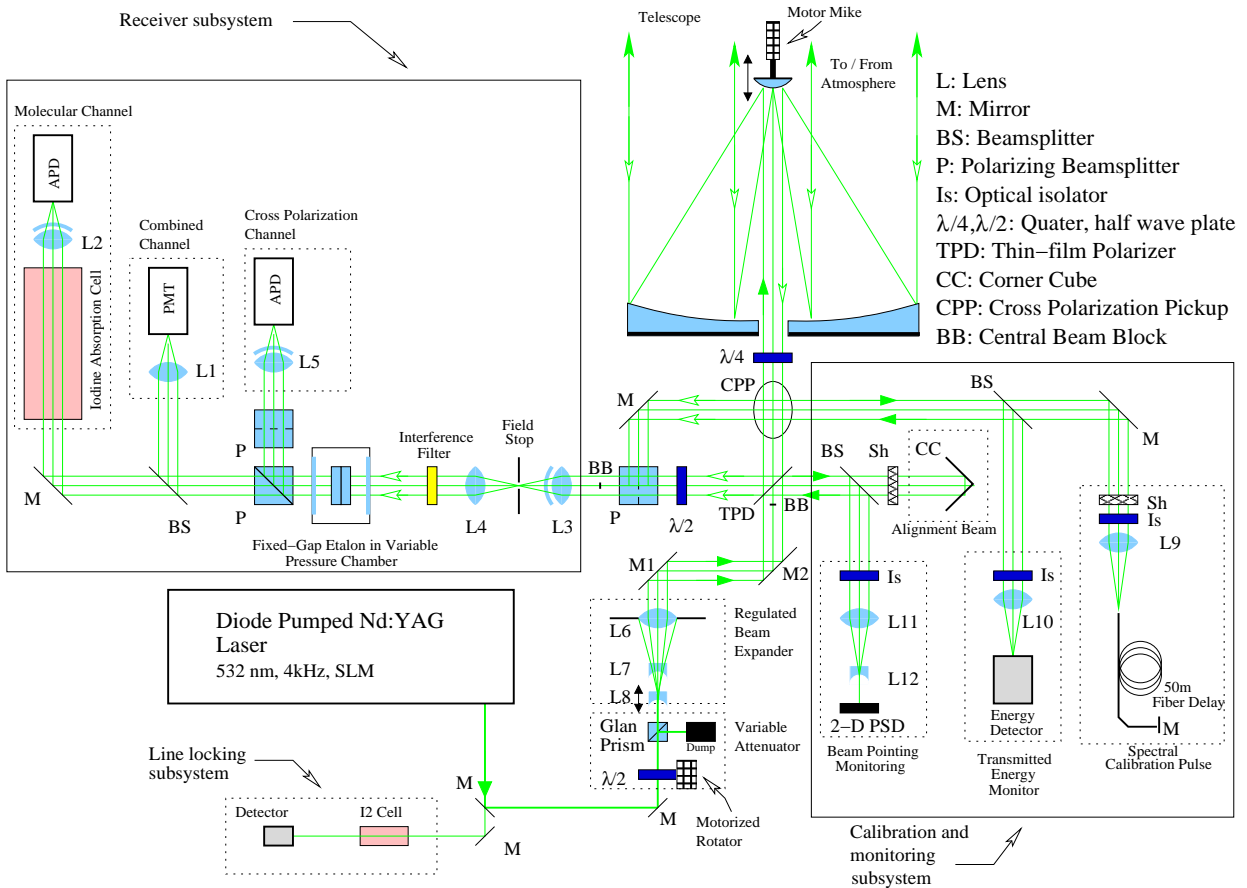


Figure 1. Schematic of the new HSRL. Mirror M2 is mounted on a stepper-motor adjusted mount. This along with feedback from the 2-d Position Sensitive Detector (PSD) allows computer control of the transmitter-receiver alignment. Small beam blocks have been installed in the transmitter beam prior to the thin-film polarizer and in the received beam prior to entry into the receiver subsystem. These were required to suppress the scattering of stray light from the transmitter into the receiver. The delay fiber in the calibration subsystem injects transmitted light into the receiver after the stray light scattered from the transmitter has disappeared. During calibration, the wavelength of the seed laser is tuned across the I_2 absorption band and the pulse injected by the fiber is used to determine the spectral response of the I_2 filter. Lens L7 expands the transmitted beam beyond the aperture of L8. Using only the central part beam provides a more uniform energy density in the transmitted beam. This allows a larger transmitted power without exceeding eyesafe limits.

Arctic locations report a large number of days with very low cloud ceilings. This is a problem for our narrow field-of-view lidar design which does not collect light from the entire transmitter illuminated area until the laser pulse is ~ 3 km from the lidar. Incomplete overlap does not effect backscatter cross section and polarization measurements because these quantities are derived from ratios of signals. However, absolute measurements of the molecular return are required to compute optical depth. The overlap function required for this measurement is obtained using a computer controlled focus adjustment on the telescope secondary mirror. A calibration sequence performed periodically during routine operation will observe the molecular lidar return while scanning the telescope focus to map the overlap function. Preliminary measurements of the geometric overlap function have been made with the system operating without the I_2 cell. These compare well with results simulated with a detailed Zemax optical model of the complete system when focus and alignment parameters in the model are varied to provide a best fit to the data. However, critical tests of stability and reproducibility await the completion of computer controlled alignment system.

		Transmitter	
Average transmitted power			0.6 W
Spectral width			< 0.1 nm
Pulse repetition rate			4 kHz
Transmitted beam divergence			$\sim 10 \mu\text{rad}$
Aperture			0.4 m
		Receiver	
Aperture			0.4 m
Angular field of view			$70 \mu\text{rad}$
Spectral bandpass			8 nm
I ₂ Blocking filter bandwidth			1.8 nm
Molecular channel detector			EG&G Geiger mode APD
Combined molecular/aerosol channel detector			Hamamatsu 7400 PMT
Crossed polarization channel detector			EG&G Geiger mode APD

Table 1: Arctic HSRL Specifications

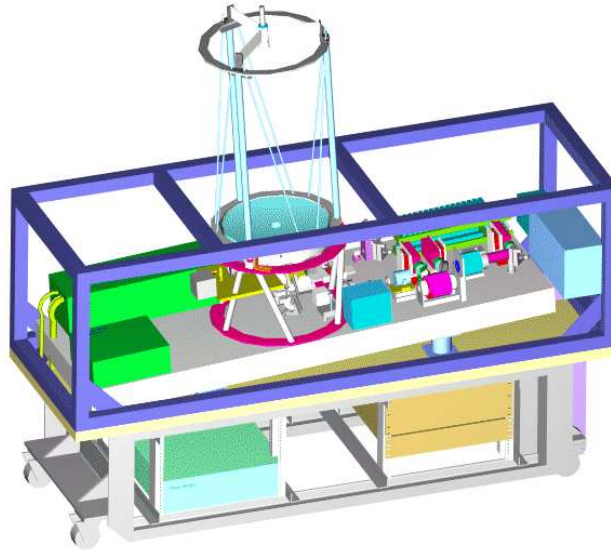


Figure 2. A perspective drawing of the arctic HSRL without its environmental enclosure. The telescope is tilted at 4° from the vertical to minimize specular reflections from oriented ice crystals.

A new PC based photon counting data system has been designed for this lidar. It consists of a master timing/control board with three accumulator boards (one each for the molecular, combined and cross-polarization channel). They employ a standard PCI computer buss. A Linux driver has been written to allow convenient access by data acquisition programs. The timing board also provides an energy monitor input which is summed along with the lidar profiles. The laser used in this lidar presents a signal with every laser pulse specifying whether the laser pulse was successfully locked to the seed laser wavelength. This indicator bit is not presented until $\sim 10 \mu\text{s}$ after the laser pulse. In order to prevent bad profiles from being added to the sum, the accumulator board buffers each profile in a FIFO memory prior to summing. If the seeded-OK bit is not asserted the profile and the associated energy monitor reading are rejected. An output FIFO memory also buffers the data transfer to the computer. The boards include an internal counter which can accommodate 50 MHz count rates. When higher count rates are needed, a 1 GHz ECL counter can be mounted on a daughter board. Each accumulator board has two sum buffers. The counter output can be directed to either of the buffers so that separate signals can be recorded when the lidar transmits alternating polarizations on successive pulses. This feature is not used on the

arctic HSRL but will be employed on our existing HSRL.

Min bin width	50 ns
Max buffer length	8192
Buffer depth	16 bits
Max accumulation interval	2048 profiles per sum
Max count rate(on board counter)	50 MHz
Max count rate(ECL counter)	1 GHz

Table 2: Data System Specifications

Testing of the new system has been slowed by late delivery of components. The data system control and accumulator cards just been delivered. These are required to implement the computer control of the system. Etalon tuning, system alignment and locking of the laser wavelength to the I_2 absorption line all require feedback from the data acquisition cards. This testing can now begin and the results will be presented at the ILRC meeting.

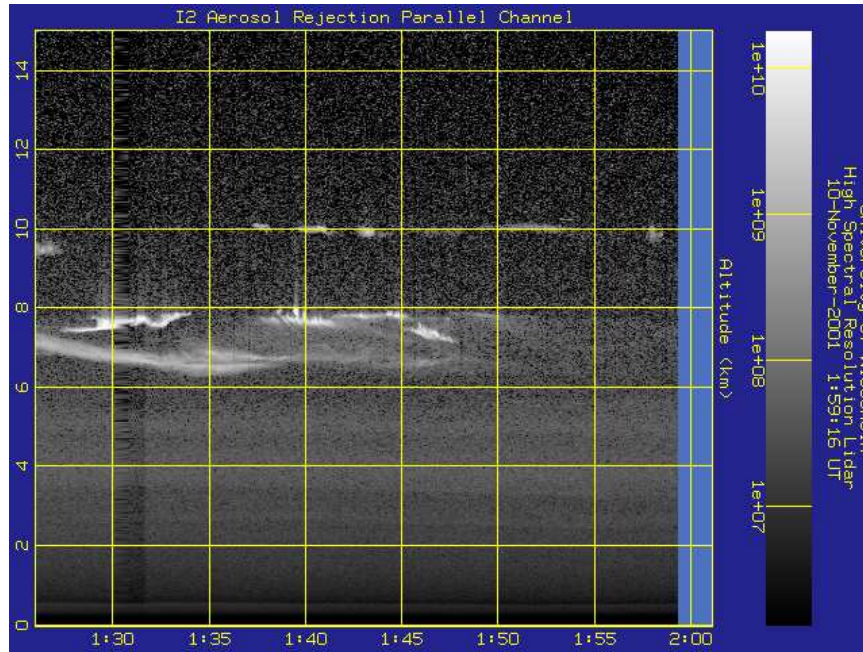


Figure 3. Data acquired with molecular channel APD detector on with the arctic HSRL. The I_2 filter was not installed for this preliminary system alignment test. Because the new data acquisition cards were incomplete, this data was acquired by patching detector outputs into the existing HSRL data system.

2. REFERENCES

1. Grund, C.J. and E. W. Eloranta, 1991: The University of Wisconsin High Spectral Resolution Lidar, *Optical Engineering*, **30**, 6-12.
2. Piironen, P. and E. W. Eloranta, 1994: Demonstration of a high-spectral-resolution lidar based on an iodine absorption filter, *Optics Letters*, **19**, 234-236.

This work was supported by NSF grant OOP-9910304.